processes

MDPI

Article

Multi-Response Modelling and Optimisation of Mechanical Properties of Al-Si Alloy Using Mixture Design of Experiment Approach

M. Poornesh [1], Shreeranga Bhat [1], E.V Gijo [2], Pavana Kumara Bellairu [1] and Olivia McDermott [3,*]

[1] Department of Mechanical Engineering, St. Joseph Engineering College, Mangalore 575028, India
[2] SQC & OR Unit, Indian Statistical Institute, Bangalore 560059, India
[3] College of Science and Engineering, University of Galway, H91 TK33 Galway, Ireland
* Correspondence: olivia.mcdermott@nuigalway.ie or olivia.mcdermott@universityofgalway.ie

Abstract: The research aims to produce, model, and optimise the mechanical properties of novel composite material through a structured multidisciplinary approach. The primary objective is to combine materials science, mechanical engineering, and statistical concepts to ensure Design for Manufacturability (DFM) from the industrial perspective. More specifically, the article is intended to determine the optimal mixture components and predictive model of Al-Si alloy with Al_2O_3 by accommodating multi-responses that enable DFM. The study adopted ASTM standards to prepare and test the novel composite material. Additionally, the Mixture Design of Experiment (DOE) approach was used to design the experimentation and subsequent analysis. In addition, microstructural images, Cox Response Trace plot, and Response Optimiser plot are effectively utilised to draw robust inferences. For multi-response modelling and optimisation, the composite material's mechanical properties, like impact strength, hardness, density, and tensile strength, are considered. The study determines that innovative composite material will yield better results when Al-Alloy is 94.65 wt% and Al_2O_3 is 5.35 wt% from a multi-responses perspective. Further, it provides predictive models with a high level of predictability. Besides, the research shows that novel composite material has better mechanical properties from a practical perspective. The article not only provides the mechanical properties of a new class of material but also shows the effective utilisation of material science and statistical concepts to develop the novel material in a structured manner. This composite material can be used as a replacement for various parts of automobiles and aircraft. Additionally, researchers can use the article's modelling and optimisation approach as a paradigm to create durable composite materials.

Keywords: multi-response; modelling; optimisation; Al-Si alloy; Al_2O_3; mixture DOE

Citation: Poornesh, M.; Bhat, S.; Gijo, E.; Bellairu, P.K.; McDermott, O. Multi-Response Modelling and Optimisation of Mechanical Properties of Al-Si Alloy Using Mixture Design of Experiment Approach. *Processes* **2022**, *10*, 2246. https://doi.org/10.3390/pr10112246

Academic Editor: Chin-Hyung Lee

Received: 10 October 2022
Accepted: 27 October 2022
Published: 1 November 2022

1. Introduction

The aerospace and automotive industries seek materials that are low in weight, have high specific strength, and can withstand wear, corrosion, cracking, fatigue, and heat, among other things [1,2]. Though conventional ferrous metals and alloys are abundant, affordable and mainly used in aerospace and automotive, they lack the properties mentioned earlier [3,4]. Thus, researchers and engineers prefer nonferrous metals like Aluminum, Magnesium and Titanium compared to ferrous metals for practical purposes. Despite its lightweight, Magnesium has a high proclivity for catching fire, making it unsuitable for use in the aerospace industry [4]. Due to its high cost, titanium is rarely used in industries [5]. As a result, Aluminium is the metal of choice in many sectors. Aluminium and its alloys are widely used in aerospace, automotive, defence, and other industries due to their lightness, strength, wear resistance, and corrosion resistance [2,6–8].

Aluminium-based composites are frequently fabricated with micro-sized ceramic powders and fibres as reinforcement. Composite materials have significantly improved strength and stiffness compared to unreinforced aluminium alloy materials. Particulates

and fibres (short and long) are usually chosen as the reinforcing particles during the preparation of the Aluminum matrix composites. The Aluminum-based metal matrix composites can be reinforced with particulates like Ti, B_2, B_4C, SiO_2, TiC, WC, BN, and ZrO_2. However, the composites made with Al_2O_3 and SiC particles have recently been investigated for various industrial applications due to their higher stability [9,10].

The composite production methods can be divided into three categories: Solid-state, Semi-solid state, and Liquid state. Powder metallurgy, mechanical alloying, and diffusion bonding are the three types of Solid-state processes [8,11]. The approach entails a series of procedures that culminate in producing particulate-reinforced Metal Matrix Composites (MMCs) from blended elemental powders before final consolidation. It enables the use of a wide variety of materials as the matrix and reinforcement. Separation effects and the production of intermetallic phases are also less common in these processes. However, this scenario's manufacturing process is relatively complex, time-consuming, costly, and energy-intensive [8,12]. The semi-solid process (SSP), which involves mixing ceramic with a matrix with solid and liquid phases, can be accomplished by various techniques, namely compocasting and thixoforging. The SSP facilitates the production of huge components while sustaining high productivity rates. The most cost-effective process for preparing MMC is liquid metallurgy. Liquid metallurgy can be divided into four categories: Pressure infiltration, Stiri casting, Spray deposition, and In situ processing. Among these, the Stir casting or Melt stirring method has several advantages over other methods. It includes a broader range of materials, improved matrix–particle bonding, easier matrix structure control, and near-net-shaped components that can be processed efficiently and cheaply, adaptable to large-scale production, and highly productive [8,13].

Naseem Ahamad et al. [7] investigated the mechanical characteristics of Al-Al_2O_3-TiO_2 composite material developed using the stir casting technique. The addition of the reinforcing particles to prepare the composite material decreased the density of the composite and increased the hardness and overall strength making it more suitable for aircraft rivets. K. Kanthavel et al. [14] studied the effects of alumina and MoS2 on the wear properties of the produced composite. The authors observed that the addition of the MoS2 acts as a solid lubricant, reducing the wear of the produced composites at high load and speed conditions. A similar trend in the results was also noticed in work done by D. Simsek et al. [15], where the Aluminium was reinforced with Al_2O_3 and graphite and in work done by Necat Altinkok [16], where the Al- alloy was mixed with α-aluminium oxide particles.

However, most of the articles in the literature followed the trial and error method in fixing and optimising the composition of the composite material components. Some researchers have recently used the Mixture Design for composite mixture optimisation [9,11,17]. This approach is based on the statistical methodology, which provides optimal mixture components and the predictive model. Further, the Mixture design facilitates multi-response optimisation, which is highly useful for engineers in the industry and ensures Design for Manufacturability (DFM) [18].

Based on the above discussion, the study's objective is to determine the optimal mixture components and predictive model of Al-Si alloy with Al_2O_3 for different mechanical properties using the Mixture design method. More specifically, research intended to study composite material's Hardness (BHN), Density (g/cm^3), Tensile (MPa) and Impact strength (J) with an optimal combination of component mixture that facilitates DFM in the industry.

2. Experimental Details

2.1. Material Selection

The present work has attempted to fabricate the composite material using the stir-casting process. As the matrix material, Al-Si alloy is chosen with chemical composition and the weight percentage being 17.95 wt% of Si, 4.23 wt% Cu, 0.58 wt% of Mg, 0.7 wt% of Fe, and 0.03 wt% of S [11]. Because of their superior resistance to wear, high strength-to-weight ratio, and less thermal expansion coefficient, Al-Si alloys are frequently used in engineering.

The reinforcing particles Al_2O_3 were obtained commercially, with a particle size varying from 60 to 80 μm [19].

2.2. Process of Fabrication

The material preparation was carried out using bottom pouring stir casting setup. The casting took place in the two-step stirring process compared to the conventional single-step process. The matrix material is completely melted by heating it above its liquid temperature. The melt is then maintained in a semi-solid state by cooling it to a midway between liquid and solidus temperature. After that, heated reinforcing granules are added and blended. Then, the melt is heated to a completely liquid state and thoroughly mixed again [20]

The graphite crucible-containing Al-Si alloy preforms were carefully placed inside the electrical furnace. The billets were then heated to 800 °C until all the metals were wholly melted and maintained at the same temperature for one hour. At this point, hexachloroethane powder was dropped into the melt, which is used as a degassing agent to remove any trapped gasses from the molten metal [21,22]. As the flux material, coarse magnesium particles are added to the mixture to increase the flowability of the reinforcing particles. The heating of the matrix material is then stopped and allowed to cool on its own to a semi-solid state. Later, the melt is heated to a temperature of 700 °C. For 30 min, the reinforcing particles are warmed to 180–200 °C to eliminate moisture and other volatile materials from the surface. The molten metal is then slowly stirred at a low speed of 200 rpm to create a vortex at the centre. To ensure that the matrix material and reinforcing particles are distributed as uniformly as possible, the reinforcements are poured into the swirl created by stirring [23]. The metal was stirred continuously for 10 min, after which the liquid slurry was poured into the mould [24].

2.3. Material Composition Selection and Design

The literature review indicated that adding the reinforcing particles to the matrix material up to 10 wt% typically produces the optimal test results [25,26]. So, the current investigation has a 0–10% limit for reinforcing particles (Al_2O_3). This suggests that the matrix material likely range between 0 to 100 wt% (Al-18 wt% Si alloy). Furthermore, tests related to the mechanical characteristics of the material (density, hardness, tensile strength, and impact strength) have been planned in a multi-response optimisation scenario. To determine the ideal material composition and perform the planned tests within the selected ranges, Minitab statistical software is used. Using Minitab statistical software, the Extreme Centroid Mixture Design technique is used to establish a composition variation matrix [27], as shown in Table 1. Three replications are added to each experimental run to reduce error during the experimentation [28].

Table 1. Experimental layout as per Mixture DOE.

Sample Number	Al-18 wt% Si	Al_2O_3
S1	100	0
S2	92.5	7.5
S3	90	10
S4	95	5
S5	97.5	2.5

2.4. Microstructure Study

The surface morphology or the microstructural analysis of the produced composite material is done according to the ASTM E8-11 standards [29]. The cut specimen surface was grinding using an emery sheet of various mesh sizes ranging from 120 to 1200. The scratches from the preceding coarse paper are removed at each grinding stage by orienting the sample perpendicular to the previous scratch site. The composite specimens were

thoroughly washed under running water to eliminate surface contamination from the previous grinding. Wet grinding is used throughout the operation to eliminate any heating-related adverse effects. Kerosene fluid was applied to the composite surface while polishing it with emery sheets to keep the abrasive particles from sticking [30,31]. The composite specimens were then polished on a velvet cloth with a smooth diamond paste in the following procedure to achieve a nearly shiny finish. Finally, the composites were etched using a Keller's reagent with 0.5 mL HF, 0.75 mL HCl, 2.5 mL HNO_3, and the rest was distilled water [31].

2.5. Hardness Test

Brinell Hardness testing was conducted to determine the composite specimens' hardness. The test was conducted according to the ASTM E10 standards [30]. The Brinell Hardness test distinguishes the material hardness by the scale of penetration on the material surface. The specimens for the tests were cut from the composite structure and polished to obtain a uniform surface finish. A hard steel ball of 5 mm in diameter is pierced on the surface of the specimen with a load of 15.6 kg/mm^2. The test was conducted multiple times on the same material surface at various locations to obtain a normalised Hardness value.

2.6. Density Test

According to the Archimedes Principle, the water displacement test is used to calculate the experimental density of the composite specimens [32], while the following equation acquires the theoretical Density.

$$\frac{1}{\rho_c} = \frac{W_m}{\rho_m} + \frac{W_r}{\rho_r} \quad (1)$$

where, ρ_c = Density of Composite Material, W_m = Weight percentage of matrix material, W_r = Weight percentage of reinforcing material, ρ_m = Density of Matrix Material, ρ_r = Density of Reinforcing Material.

2.7. Tensile Test

The tensile test determines a material's ability to withstand a static load in tension. The tensile test is conducted according to the ASTM E-8 standard using a computerised universal testing machine and averaged over 5 test readings [33].

2.8. Impact Test

The impact strength of the composite specimens is computed using a V-notched impact specimen following the Charpy test conditions. The test specimens are prepared with the ASTM E23 standards [34].

The above tests were conducted on the produced composite materials as per the Mixture DOE experimental layout (Figure 1) for a minimum of three times to accommodate any experimental errors. All four properties, viz density, tensile strength, impact strength, and hardness, are analysed with Minitab statistical software in the Mixture Design environment to identify the optimal mixture combination. Thus, a statistically fit model that satisfies the multi-response optimisation criteria will lead to numerous benefits for Research and Development (R&D) activities and DFM [17,18].

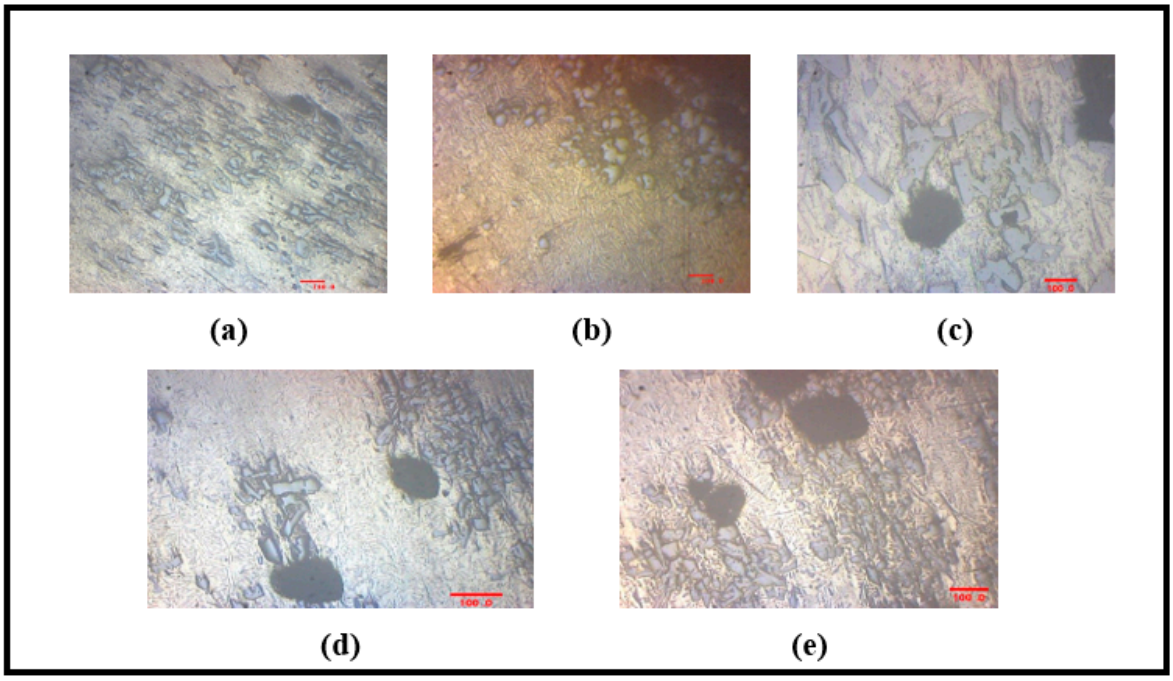

Figure 1. Microstructural Images at 100× magnification of the Composite Materials reinforced with (**a**) 0 wt% (**b**) 2.5 wt% (**c**) 5 wt% (**d**) 7.5 wt% (**e**) 10 wt% of Al_2O_3.

3. Results

3.1. Microstructure

Figure 1 shows the optical microstructural images of the composites reinforced with Al_2O_3 particles according to the composition mentioned in Table 1. The distribution of the reinforcing particles is one of the significant factors in fabricating metal matrix composites.

The microstructural images show that the reinforcing particles are almost distributed uniformly throughout the matrix. As the percentage of the reinforcing particles increases in the matrix, particle agglomeration can be observed in certain areas.

Figure 1a shows the unreinforced composite specimen. The microstructural image reveals that the Al-Si matrix material consists of α-Al dendric particles or needle-shaped eutectic Si particles and huge clusters of primary silicon particles. The Al_2O_3 particles can be seen as the dark black region, which increases with the increase in the content. It can be noted that there are no noticeable gaps between the matrix and the reinforcing particles, which proves an excellent bonding between the matrix and reinforcements. Adding Magnesium particles has also helped provide a stable bond between the matrix and reinforcements by increasing the wettability of the reinforcing particles.

The Al_2O_3 particles react with the Mg particles through the following reaction [35,36]:

$$M_g + \frac{4}{3}AL_2O_3 \rightarrow M_gAL_2O_4 + \frac{2}{3}Al \quad (2)$$

The resulting compound, Magnesium aluminate, has been discovered to successfully enhance composites' hardness and strength, which will be evident in hardness and Ultimate Tensile Strength results [37].

3.2. Hardness

Figure 2a shows the Brinell Hardness Number (BHN) variation because of the reinforcement percentage variation. To help lower discrepancy, the composite results have been generated from the overall mean of 5 trials. It is clear from Figure 2a that the composites' hardness increases due to the addition of the reinforcing particles. The unreinforced composite has the lowest hardness number, with an average value of 24 BHN. In contrast, the

highest hardness value is obtained for composite with 10 wt% of reinforcing particles with an average hardness of 33 BHN.

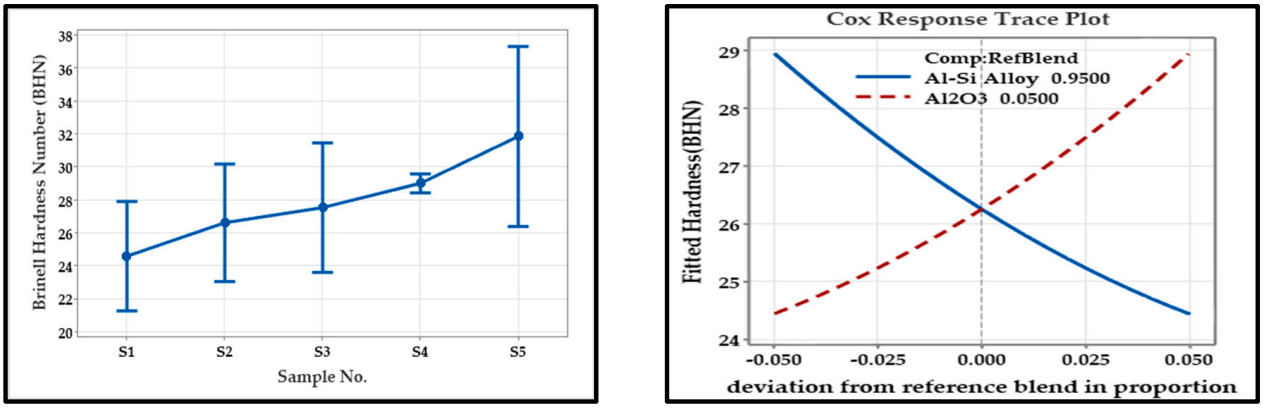

(a) **(b)**

Figure 2. Brinell Hardness Number and Cox Response Trace plot of the Composite Material. (**a**) Hardness; (**b**) Cox Response Trace.

Additionally, for the parameter under consideration, a Cox plot was created better to understand each component's impact on the response. With the help of an illustrative line from the reference blend to the vertex, the figure shows the effects of changing a component. Figure 2b gives the Cox Response Plot for the hardness of the composite. It can be seen from the plot that the proportion of Al_2O_3 is positively correlated to hardness, and Al-Alloy is negatively correlated to hardness. In other words, it means that the addition of the Al_2O_3 particles will have a significant and positive influence on the overall hardness of the composite material produced.

The unreinforced composite will probably be less hard because there are not any hard ceramic reinforcing particles in it, and they tend to encounter plastic deformation due to external indentation. In general, ceramic particles are inherently hard due to the presence of both covalent and ionic bonds. The ionic bonds in the ceramic particles make them very rigid and hard. Thus, breaking these particles would require a large amount of energy. The addition of the hard ceramic particles enhances the bonding with the soft matrix material, thus arresting any plastic deformation that implicitly increases the hardness of the material [38]. The microstructural images of the produced composite specimens (Figure 1) clearly showed an excellent intermolecular bonding between the matrix and reinforcing particles. This proves that the indentation loading to cause the deformation was avoided, thus increasing the hardness of the composite.

In addition, Orowan's Theory suggests that due to the thermal mismatch mechanism and the load-bearing ability of the ceramic particles, there will be an increase in the hardness at the interface of the matrix and reinforcing material [39].

3.3. Density

Figure 3a illustrates the variation in the composite material density. It increases with the increase in the amount of reinforcing particles. This increase in the Density of the composites is attributed to the high Density of the reinforcing particles. The reinforcement, Al_2O_3 particles, have a high density of 3.98 g/cc, whereas the matrix material has a density of 2.64 g/cc. Moreover, as the amount of reinforcing particles in the matrix increases, so does the density. Besides, it can be observed that there is a 4.2% increase in density value when the matrix is reinforced with 10 wt% of Al_2O_3 particles compared with the unreinforced material. From the Cox plot of Density shown in Figure 3b, it can be seen that, similar to hardness, there is a positive correlation between Density due to Al_2O_3 and

a negative correlation due to Al-Alloy. As explained, the density of the composite increases due to the addition of the reinforcing particles and the statistical analysis, which depicts the same.

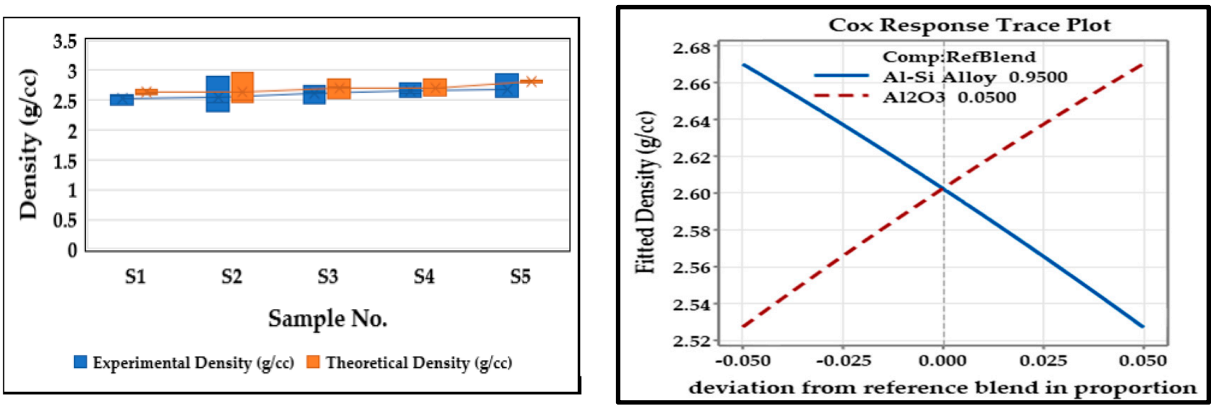

(**a**) (**b**)

Figure 3. Variation of Density due to the reinforcing particles and Cox trace plot. (**a**) Density; (**b**) Cox Response Trace.

The trend observed in the results can be explained by two key concepts, (1) the Density of the particles involved in the preparation and (2) the porosity in the composite due to manufacturing. The first concept explains that increasing or decreasing the composite's final value relies on the matrix's density and the reinforcing particles. Furthermore, the second concept suggests that there will always be a decrease in the density of the composite material due to the presence of pores or voids in the fabricated composites. These pores and voids are primarily due to particle agglomeration or poor wettability [40].

In the current study, it is evident from the experimental density values that the composite density increases due to the inclusion of high-density reinforcing particles, as suggested in the first concept. When comparing theoretical and experimental density values, it can be noted that the theoretical values are higher than the experimental values. This difference is due to voids or porosity in the produced composite material. It is because, when casting, particles usually enter the melt as a group, entombing air among them to form a void space [41].

3.4. Tensile Test

Figure 4a shows the reinforcing particles' influence on the composite material's tensile strength. As the percentage of reinforcing particles increases, the tensile strength increases proportionally, indicating the positive impact of adding reinforcing particles. Further, it is observed from Figure 4b that the tensile strength of the composite material has been found to have a negative correlation with the Al-alloy and a positive correlation with reinforcing Al_2O_3 particles.

The dislocation density, resistance offered by the reinforcing particles on the plastic flow, and dislocation interaction are factors that highly influence the composite materials' strain hardening. Apart from these, induced thermal stress at the matrix interface and reinforcing particles, due to the difference in their thermal expansion coefficient, can also be the leading cause of the improvement in strength [2].

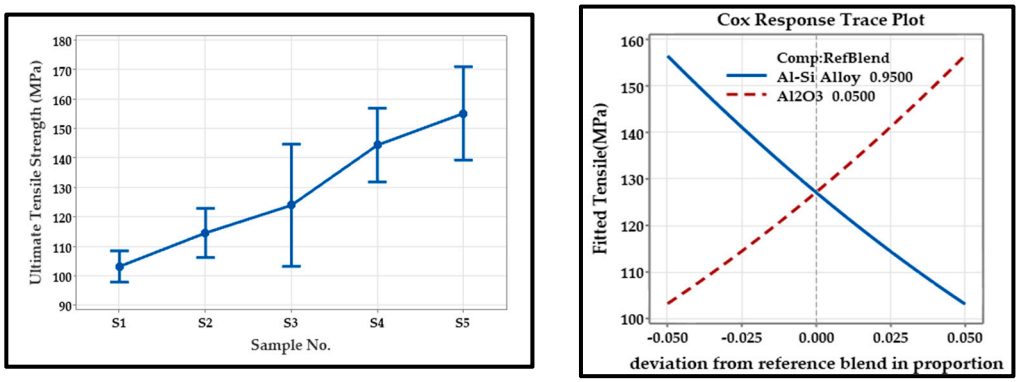

(**a**) (**b**)

Figure 4. Influence of reinforcements on Tensile Strength. (**a**) Tensile Strength; (**b**) Cox Response Trace.

Figure 4 clearly shows that the Al_2O_3 particles' inclusion causes a noticeable rise in the Tensile Strength. Compared with the unreinforced matrix material, the composite with 10 wt% reinforcing particles has a strength in the range of 163 MPa, which is 57% higher. As seen in the results of the hardness test, due to the changes in the thermal stress in the matrix and reinforcements, there are chances that the dislocation density within the matrix increases, which in turn improves the strength of the matrix, thereby that of the fabricated composite [39,42].

It is evident from Figure 5a that the reinforcing particles' presence considerably reduces the composite specimen's impact strength. The Charpy test conducted to find the impact strength of the composite specimens revealed that the addition of the reinforcing particles leads to its reduction. Unlike the other Cox Response Trace plot established for mechanical properties, in the case of Impact Strength, it can be seen that the positive correlation is found in Al-alloy, and a negative correlation is obtained due to Al_2O_3, as observed in Figure 5b.

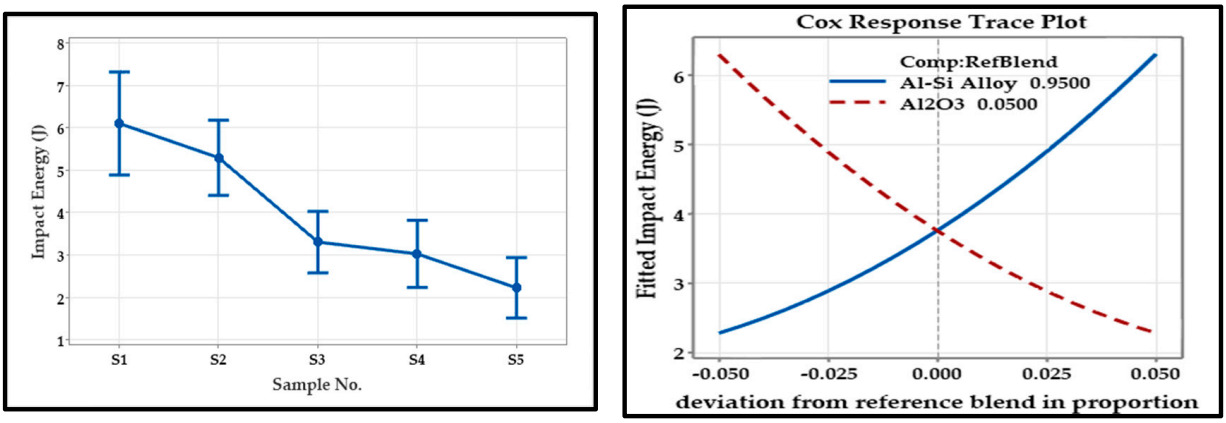

(**a**) (**b**)

Figure 5. Variation of Impact Energy with reinforcing particles. (**a**) Impact Energy; (**b**) Cox Response Trace.

The unreinforced matrix material is found to have high impact energy compared to the reinforced composites. The matrix material used in the study is inherently ductile, thus leading to plastic deformation at room temperature [34]. Adding ceramic reinforcing particles reduces the composite's ability to absorb the energy. This is mainly due to the formation of high-stress concentration areas. When the reinforcing particles increase, particle isolation becomes almost impossible within this ductile matrix. Hence, crack propagation becomes easy, leading to a quick failure [43].

3.5. Predictive Modelling

A regression analysis was carried out to establish the predicted model for the mechanical parameters under examination. In the initial stages of this regression analysis, a model summary for all the mechanical properties is acquired. Table 2 provides the predictive model, and Table 3 summarises the model. Table 3 provides the robustness and predictability of the model. From Table 3, the R-sq (adj) values indicate a 95.55% variation in Hardness, 86.09% variation in Density, 98.46% variation in Tensile strength, and the predictive model describes a 93.96% variation in Impact Energy. This high R-sq (adj) value demonstrates how well the model fits the observed values. Furthermore, the high R-sq (pred) value indicates a high level of predictability. This assures the acceptability of the established predictive models.

Table 2. Predictive models.

Hardness (BHN) = 229.7 − (2.052 A) − (0.01779 A × B)
Density (g/cc) = 2.59 − (0.0006 A) + (0.000152 A × B)
Tensile (MPa) = 1611 − (15.08 A) − (0.1082 A × B)
Impact Energy (J) = 158.0 − (1.517 A) − (0.02133 A × B)

Note: A = Al-Si Alloy; B = Al_2O_3.

Table 3. Model summary for predictability.

Property	S	R-sq	R-sq (adj)	R-sq (pred)
Hardness (BHN)	0.357663	96.18%	95.55%	93.95%
Density (g/cc)	0.0208375	88.08%	86.09%	83.44%
Tensile (Mpa)	2.44600	98.68%	98.46%	98.14%
Impact Energy (J)	0.376534	94.82%	93.96%	92.42%

3.6. Multi-Response Optimisation

In order to identify the optimal mixture component of all the mechanical properties involved, it addresses the objectives of being either Maximum or Minimum. It is defined within the data framework, as observed in Table 4. From the standpoint of DFM and industrial applications, it is possible to "weight" and "importance for every mechanical property or response under consideration while performing a multi-response optimisation study using the Minitab software. For the current study, both the weight and importance are considered equal for all the responses and are presented in Table 4. The term "weight" estimates the desirability pattern of the interval between the lower (or higher) bound and the target. In order to achieve the target value, the weight can be reset between 0.1 and 10 by either emphasising it or de-emphasising it [27]. The term "importance" signifies the relative importance of the variables used during the multi-response optimisation. It also represents the effect each response holds on the composite desirability. The range of values used in the case of importance should be between 0.1 and 10. In any case, where all the responses are treated equally, it can be set as 1. If the responses are given various values, then the response with a larger value is considered more important than the other [27,44]. Additionally, a Response Optimiser Plot is generated to correlate with the output values computed and presented in Table 5.

Table 4. Optimisation Parameter.

	Objective	Minimum	Target	Maximum	Weightage	Importance
H (BHAN)	Maximum	24.20	29.33	29.33	1	1
T (MPa)	Maximum	102.40	155.70	155.70	1	1
D (g/cc)	Minimum	2.52	2.52	2.69	1	1
I (J)	Maximum	2.00	6.40	6.40	1	1

Note: H = Hardness; T = Tensile Strength; D = Density; I = Impact Energy.

Table 5. Local Solution.

Local Solutions	Component Proportion		Mechanical Properties		Individual Desirability	Composite Desirability
	Al-Si Alloy	Al_2O_3				
1	94.65	5.35	H (BHN)	26.410	0.430795	0.442718
			T (MPa)	128.969	0.498472	
			D (g/cc)	2.607	0.485794	
			I (J)	3.620	0.368252	
2	90	10	H (BHN)	28.948	0.925610	0.287936
			T (MPa)	156.466	1.000000	
			D (g/cc)	2.670	0.116695	
			I (J)	2.280	0.063636	
3	100	0	H (BHN)	24.438	0.046338	0.153430
			T (MPa)	103.079	0.012740	
			D (g/cc)	2.527	0.959048	
			I (J)	6.307	0.978788	

Note: H = Hardness; T = Tensile Strength; D = Density; I = Impact Energy.

Individual desirability and Composite Desirability values are used to identify the best possible solution that will eventually improve all the responses. Individual Desirability is used when the optimisation is done for a single response. In contrast, Composite Desirability is used when the optimisation is done for a set of overall responses. Composite desirability represented by D helps determine how well settings optimise a set of responses in general. The range used for desirability is usually between 0 to 1. When the value of 0 is obtained, it implies that a few responses may be outside the acceptable limits, while 1 represents an ideal case. When experimentation needs to accept and address multiple responses, a factor setting rarely maximises the desirability of all responses simultaneously. Thus, Minitab software usually maximises the composite desirability. By emphasising the response, which is most important, the composite desirability brings together all the individual desirability values into a single measure. When the composite desirability value is closer to 1, it indicates that all the responses will achieve favourable results [44].

Table 5 gives information about the local solutions obtained or, in other words, the possible solution that helps in defining the optimal solution based on the maximum composite desirability. This maximum value needs closer to 1, which points toward the component set that helps achieve the promising result for all the properties. Further, Figure 6 and Table 5 show that the composite material prepared with Al-alloy or the matrix material = 94.65 wt% and Al_2O_3 = 5.35 wt% has the highest composite desirability value of D = 0.442718 will give the best results. Thus, these compositions were selected as the best composition to improve all the mechanical properties.

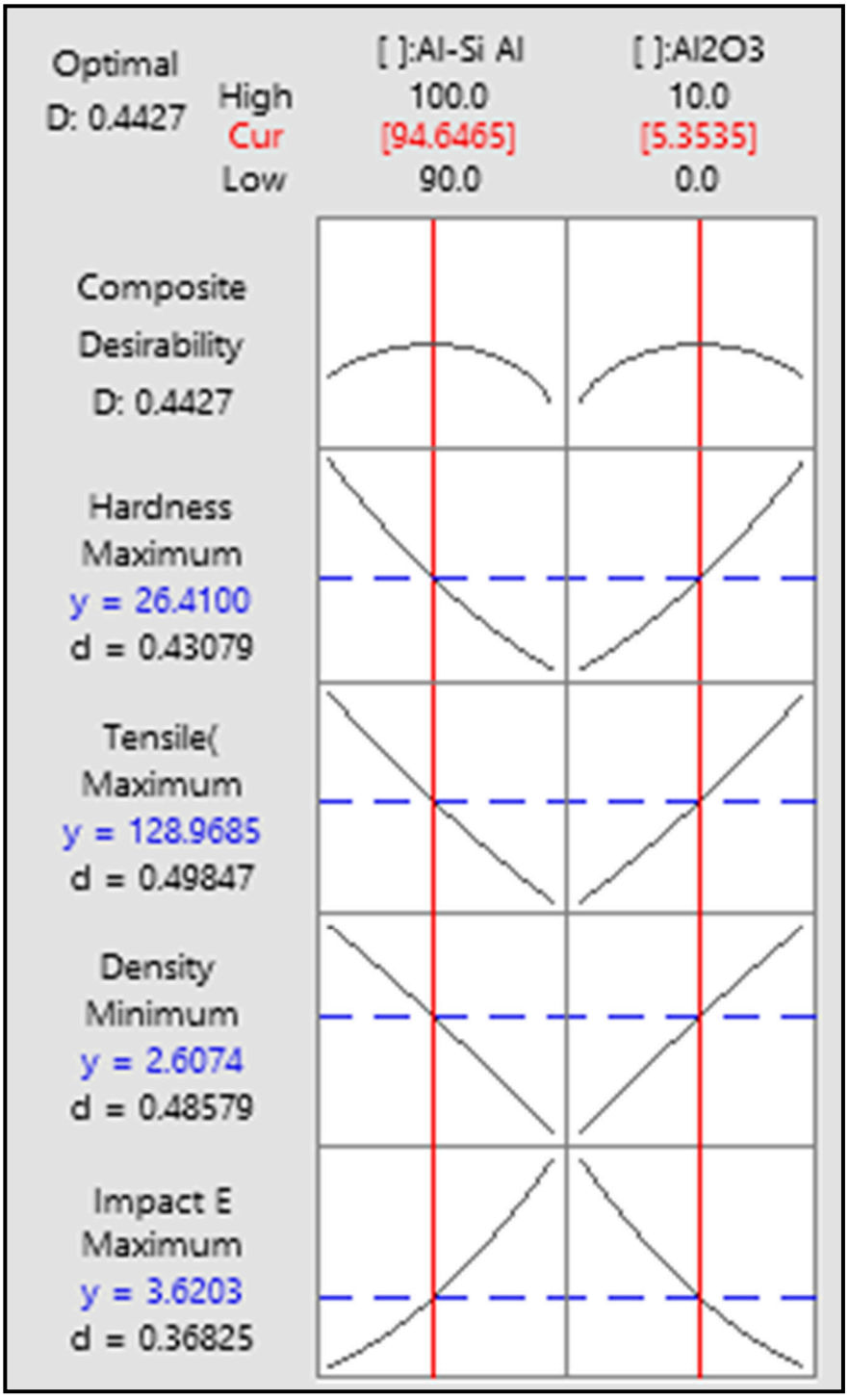

Figure 6. Response Optimiser Plot.

3.7. Validation of the Predictive Model

The next step is to validate the results and confirm the robustness of the regression equation. The predicted value for each objective is computed using the established equation, as shown in Table 2. Subsequently, the composite material was prepared using the optimal material combination (Al-Alloy = 94.65 wt% and Al_2O_3 = 5.35 wt%) from the Multi Response study. The composite material was prepared using the same material combination and operating conditions three times, and the properties of each were tested multiple times. An average result was considered for validation to maintain non-linearity

and avoid bias and errors. Finally, the Absolute Relative Deviation (ARD) is computed, which gives the degree of predictability according to the following equation:

$$\text{ARD}(\%) = \frac{Observed - Fit}{Observed} \times 100$$

Table 6 gives the overview of predicted, observed and ARD, where it can be seen that ARD is the minimum among all the mechanical properties under consideration for the study [11,17]. With this, it can be confirmed that the predictability of the regression equations generated is robust. Nevertheless, minor variations in the results can be observed due to certain unavoidable noise factors.

Table 6. Predicted and observed response of the optimal mixture components.

	Predicted Values		Observed Values				Absolute Relative Deviation (ARD) (%)
Responses	**Fit**	**95% Predictive Interval (PI)**	**Observation-1**	**Observation-2**	**Observation-3**	**Average**	
H (BHN)	26.4	(25.6, 27.3)	26.6	26.7	26.5	26.6	0.8
D (g/cc)	2.6	(2.6, 2.7)	2.6	2.7	2.7	2.7	2.5
T (MPa)	129	(123.2, 134.7)	127	131	130	129.3	0.3
I (J)	3.6	(2.7, 4.5)	3.7	3.7	3.6	3.7	1.8

Note: H = Hardness; T = Tensile Strength; D = Density; I = Impact Energy.

4. Conclusions

The research established a well-defined multidisciplinary methodology based on mechanical engineering, material engineering, and statistical methodologies. This methodology helped to develop composite materials and validate the mechanical properties of the materials with the optimal utilisation of available resources. Furthermore, the research shows that the Mixture Design technique enables precise optimisation of mixture components in multi-response scenarios and aids in developing better predictive models.

- The results obtained through the statistical analysis showed that both Al alloy and the reinforced Al_2O_3 particles significantly influence the composite material. Moreover, a positive correlation was observed in the mechanical properties such as hardness, tensile strength and density. In contrast, the impact strength of the composite material was negatively correlated and vice versa.
- The microstructural analysis of the produced composite materials suggested that though the reinforcing particles were mixed uniformly by creating a centre vortex while stirring, there existed a non-uniform settlement of the particles among the matrix material. The existence of the primary silicon particles, eutectic silicon particles in the form of needles and the Al_2O_3 particles were noticed in the images.
- The reinforcing particles' inclusion in the composite material preparation proved beneficial. Most mechanical properties, such as density, hardness, and tensile strength, have shown a positive increase in the values. With the predictive model, the mechanical properties obtained were almost in line with the values obtained through the regression equations, thus rendering the equations obtained as accurate. Thus, the study finds that the composite material produced with Al-Alloy = 94.65 wt% and Al_2O_3 = 5.35 wt% leads to the best results.

From a DFM and industrial standpoint, the current research delved in depth to create a multidisciplinary technique to develop, forecast, and optimise the composition of the produced material. Although multi-responses are acclimated into the study, the researchers firmly believe that to enhance the knowledge base and get a better insight into the behaviour of the newly developed composite material, the study needs to be extended to other properties like tribological, vibration as well as thermal. These studies will help industry and academia achieve these composite materials' potential for societal benefit.

Author Contributions: Conceptualisation, M.P., S.B., E.V.G., P.K.B. and O.M.; methodology, M.P., S.B. and E.V.G.; formal analysis, M.P., S.B., E.V.G. and P.K.B.; writing—original draft preparation, M.P., S.B., E.V.G., P.K.B. and O.M.; writing—review and editing, S.B., P.K.B. and O.M.; supervision, O.M. and S.B.; project administration, M.P. All authors have read and agreed to the published version of the manuscript.

Funding: This research received no external funding.

Data Availability Statement: Not applicable.

Conflicts of Interest: The authors declare no conflict of interest.

References

1. Włodarczyk-Fligier, A.; Dobrzański, L.; Kremzer, M.; Adamiak, M. Manufacturing of Aluminium Based Composite Materials Reinforced by Al2O3 Particles. *J. Achiev. Mater. Manuf. Eng.* **2008**, *27*, 99–102.
2. Akbari, M.K.; Baharvandi, H.R.; Mirzaee, O. Investigation of particle size and reinforcement content on mechanical properties and fracture behavior of A356-Al_2O_3 composite fabricated by vortex method. *J. Compos. Mater.* **2014**, *48*, 3315–3330. [CrossRef]
3. Poornesh, M.; Saldanha, J.X.; Singh, J.; Pinto, G.; Gaurav, M. Comparison of mechanical properties of coconut shell ash and SiC reinforced hybrid aluminium metal matrix composites. *Am. J. Mater. Sci.* **2017**, *7*, 116–119.
4. Fentahun, M.A.; Savas, M.A. Materials Used in Automotive Manufacture and Material Selection Using Ashby Charts. *Int. J. Mater. Eng.* **2018**, *8*, 40–54.
5. Adam, G.; Zhang, D.L.; Liang, J.; Macrae, I. A Novel Process for Lowering the Cost of Titanium. In *Advanced Materials and Processing IV*; Trans Tech Publications Ltd.: Bach, Switzerland, 2007; pp. 147–152.
6. Koli, D.K.; Agnihotri, G.; Purohit, R. Advanced Aluminium Matrix Composites: The Critical Need of Automotive and Aerospace Engineering Fields. *Mater. Today Proc.* **2015**, *2*, 3032–3041. [CrossRef]
7. Ahamad, N.; Mohammad, A.; Sadasivuni, K.K. Phase, microstructure and tensile strength of Al–Al_2O_3–C hybrid metal matrix composites. *Proc. Instit. Mech. Eng. Part C J. Mech. Eng. Sci.* **2020**, *234*, 1–13. [CrossRef]
8. Kumar Sharma, A.; Bhandari, R.; Aherwar, A.; Pinca-Bretotean, C. A study of fabrication methods of aluminum based composites focused on stir casting process. *Mater. Today Proc.* **2020**, *27*, 1608–1612. [CrossRef]
9. Poornesh, M.; Bhat, S.; Gijo, E.V.; Bellairu, P.K. Enhancing the tensile strength of SiC reinforced aluminium-based functionally graded structure through the mixture design approach. *Int. J. Struct. Integr.* **2022**, *13*, 150–163. [CrossRef]
10. Srinivas, P.N.S.; Babu, P.R.; Balakrishna, B. Material characterisation and optimisation of CNT-reinforced aluminum (AA7075) functionally graded material processed by ultrasonic cavitation. *Funct. Compos. Struct.* **2020**, *2*, 1–13. [CrossRef]
11. Poornesh, M.; Bhat, S.; Gijo, E.V.; Bellairu, P.K. Multi-objective modelling and optimisation of Al–Si–SiC composite material: A multidisciplinary approach. *Multiscale Multidiscip. Model. Exp. Des.* **2022**, *5*, 53–66. [CrossRef]
12. Dadkhah, M.; Dadkhah, M.; Mosallanejad, M.H.; Iuliano, L.; Saboori, A. A Comprehensive Overview on the Latest Progress in the Additive Manufacturing of Metal Matrix Composites: Potential, Challenges, and Feasible Solutions. *Acta Metall. Sin. Engl. Lett.* **2021**, *34*, 1173–1200. [CrossRef]
13. Singh, H.; Singh, G.; Singh, K.; Vardhan, S. Evaluation of mechanical performance on a developed AA 6061matrix-Mg/0.9-Si/0.68 reinforced with B_4C based composites. *Funct. Compos. Struct.* **2021**, *3*, 1–10. [CrossRef]
14. Kanthavel, K.; Sumesh, K.R.; Saravanakumar, P. Study of tribological properties on Al/Al_2O_3/MoS_2 hybrid composite processed by powder metallurgy. *Alex. Eng. J.* **2016**, *55*, 13–17. [CrossRef]
15. Şimşek, D.; Şimşek, İ.; Özyürek, D. Relationship between Al_2O_3 Content and Wear Behavior of Al+2% Graphite Matrix Composites. *Sci. Eng. Compos. Mater.* **2020**, *27*, 177–185. [CrossRef]
16. Altinkok, N. Use of Artificial Neural Network for Prediction of Mechanical Properties of α-Al_2O_3 Particulate-reinforced Al–Si10Mg Alloy Composites Prepared by using Stir Casting Process. *J. Compos. Mater.* **2006**, *40*, 779–796. [CrossRef]
17. Bellairu, P.K.; Bhat, S.; Gijo, E.V.; Mangalore, P. Multi-Response Modelling and Optimization of Agave Cantala Natural Fiber and Multi-wall Carbon Nano Tube Reinforced Polymer Nanocomposite: Application of Mixture Design. *Fibers Polym.* **2022**, *23*, 1089–1099. [CrossRef]
18. Bellairu, P.K.; Bhat, S.; Gijo, E.V. Modelling and optimisation of natural fibre reinforced polymer nanocomposite: Application of mixture-design technique. *Multidiscip. Model. Mater. Struct.* **2021**, *17*, 507–521. [CrossRef]
19. Agrawal, A.; Satapathy, A. Effect of Al_2O_3 Addition on Thermo-Electrical Properties of Polymer Composites: An Experimental Investigation. *Polymer Compos.* **2014**, *36*, 102–112. [CrossRef]
20. Madhukar, P.; Selvaraja, N.; Rao, C.S.P.; Kumar, G.B.V. Fabrication and characterisation two step stir casting with ultrasonic assisted novel AA7150-hBN nanocomposites. *J. Alloys Compd.* **2020**, *815*, 1–12. [CrossRef]
21. Mangalore, P.; Vittal, C.S.; Akash, U.A.; Abhiram, S.; Advaith, J. Study of tribological properties of Al 7079 alloy reinforced with agro waste particles. *AIP Conf. Proc.* **2019**, *2080*, 20–29.
22. Grilo, J.; Carneiro, V.H.; Teixeira, J.C.; Puga, H. Manufacturing Methodology on Casting-Based Aluminium Matrix Composites: Systematic Review. *Metals* **2021**, *11*, 436–445. [CrossRef]

23. Gowda, K.P.; Prakash, J.N.; Gowda, S.; Babu, B.S. Effect of Particulate Reinforcement on the Mechanical Properties of Al2024-WC MMCs. *J. Miner. Mater. Charact. Eng.* **2015**, *3*, 469–476. [CrossRef]
24. Sambathkumar, M.K.; Navaneetha, P.K.; Ponappa, K.; Sasikumar, K.S.K. Mechanical and Corrosion Behavior of Al7075 (Hybrid) Metal Matrix Composites by Two Step Stir Casting Process. *Latin Am. J. Solids Struct.* **2017**, *14*, 243–255. [CrossRef]
25. Sharma, P.; Dabra, V.; Dwivedi, S.P. Wear characteristics of AA2014/10 wt% Al_2O_3 reinforced AMCs. *Mater. Today Proc.* **2020**, *25*, 931–933. [CrossRef]
26. Yehia, H.M.; Allam, S. Hot Pressing of Al-10 wt% Cu-10 wt% Ni/x (Al_2O_3–Ag) Nanocomposites at Different Heating Temperatures. *Met. Mater. Int.* **2021**, *27*, 500–513. [CrossRef]
27. Arnold, S.F. Design of Experiments with MINITAB. *Am. Stat.* **2006**, *60*, 205. [CrossRef]
28. Peruggia, M. Experiments with Mixtures: Designs, Models, and the Analysis of Mixture Data. *J. Am. Stat. Assoc.* **2003**, *98*, 259.
29. Chen, J.; Wen, F.; Liu, C.; Li., W.; Zhou, Q.; Zhu, W.; Zhang, Y.; Guana, R. The microstructure and property of Al-Si alloy improved by the Sc-microalloying and Y_2O_3 nano-particles. *Sci. Technol. Adv. Mater.* **2021**, *22*, 205–217. [CrossRef]
30. Imran, M.; Khan, A.R.A.; Megeri, S.; Sadik, S. Study of hardness and tensile strength of Aluminium-7075 percentage varying reinforced with graphite and bagasse-ash composites. *Resour.-Eff. Technol.* **2016**, *2*, 81–88. [CrossRef]
31. Singh, J.; Jawalkar, C.S.; Belokar, R.M. Analysis of Mechanical Properties of AMC Fabricated by Vacuum Stir Casting Process. *Silicon* **2020**, *12*, 2433–2443. [CrossRef]
32. Akinwamide, S.O.; Abe, B.T.; Akinribide, O.J.; Obadele, B.A.; Olubambi, P.A. Characterization of microstructure, mechanical properties and corrosion response of aluminium-based composites fabricated via casting—A review. *Int. J. Adv. Manuf. Technol.* **2020**, *109*, 975–991. [CrossRef]
33. Du, Z.; Chen, H.C.; Tan, M.J.; Bi, G.; Chua, C.K. Investigation of porosity reduction, microstructure and mechanical properties for joining of selective laser melting fabricated aluminium composite via friction stir welding. *J. Manuf. Processes* **2018**, *36*, 33–43. [CrossRef]
34. Ozden, S.; Ekici, R.; Nair, F. Investigation of impact behaviour of aluminium based SiC particle reinforced metal–matrix composites. *Compos. Part A Appl. Sci. Manuf.* **2007**, *38*, 484–494. [CrossRef]
35. Hashishin, T.; Kodera, Y.; Yamamoto, T.; Ohyanagi, M.; Munir, Z.A. Synthesis of (Mg, Si)Al2O4 Spinel from Aluminum Dross. *J. Am. Ceram. Soc.* **2008**, *87*, 496–499. [CrossRef]
36. El-Aziz, K.A.; Saber, D.; Sallam, H.E.D.M. Wear and Corrosion Behavior of Al–Si Matrix Composite Reinforced with Alumina. *J. Bio-Tribo-Corros.* **2015**, *1*, 1–10. [CrossRef]
37. Liao, H.; Zhan, M.; Li, C.; Ma, Z.; Du, J. Grain refinement of Mg-Al alloys inoculated by $MgAl_2O_4$ powder. *J. Magnes. Alloys* **2021**, *9*, 1211–1219. [CrossRef]
38. Bandil, K.; Vashisth, H.; Kumar, S.; Verma, L.; Jamwal, A.; Kumar, D.; Singh, N.; Sadasivuni, K.K.; Gupta, P. Microstructural, mechanical and corrosion behaviour of Al–Si alloy reinforced with SiC metal matrix composite. *J. Compos. Mater.* **2019**, *53*, 4215–4223. [CrossRef]
39. Zhang, J.; Chen, Z.; Zhao, J.; Jiang, Z. Microstructure and mechanical properties of aluminium-graphene composite powders produced by mechanical milling. *Mech. Adv. Mater. Modern Processes* **2018**, *4*, 1–9. [CrossRef]
40. Prabhu, T.; Murugan, M.; Chiranth, B.P.; Mishra, R.K.; Rajini, N.; Marimuthu, P.; Babu, D.P.; Suganya, G. Effects of Dual-Phase Reinforcement Particles (Fly Ash + Al_2O_3) on the Wear and Tensile Properties of the AA 7075 Al Alloy Based Composites. *J. Inst. Eng. Ser. D* **2019**, *100*, 29–35. [CrossRef]
41. Ajagol, P.; Anjan, B.N.; Marigoudar, R.N.; Kumar, G.V.P. Effect of {SiC} Reinforcement on Microstructure and Mechanical Properties of Aluminum Metal Matrix Composite. *IOP Conf. Ser. Mater. Sci. Eng.* **2018**, *376*, 1–9. [CrossRef]
42. Ezatpour, H.R.; Sajjadi, S.A.; Sabzevar, M.H.; Huang, Y. Investigation of microstructure and mechanical properties of Al6061-nanocomposite fabricated by stir casting. *Mater. Des.* **2014**, *55*, 921–928. [CrossRef]
43. Daniel-Mkpume, C.C.; Okonkwo, E.G.; Aigbodion, V.S.; Offor, P.O.; Nnakwo, K.C. Silica sand modified aluminium composite: An empirical study of the physical, mechanical and morphological properties. *Mater. Res. Express IOP Publ.* **2019**, *6*, 1–13. [CrossRef]
44. Montgomery, D.C. *Design and Analysis of Experiments*, 9th ed.; Wiley: New York, NY, USA, 2017.